

Seasonal variability of thermal fronts in the Southwestern Arafura Sea in El Niño dan La Niña

Nabila N. Hanifah^{1*}, I Wayan Nurjaya², Yuli Naulita², Nyoman M. N. Natih².

¹Magister program in Marine Sciences, Faculty of Fisheries and Marine Sciences, IPB University, 16680, Bogor, Indonesia

²Marine Sciences, Faculty of Fisheries and Marine Sciences, IPB University, 16680, Bogor, Indonesia

Abstract. Sea surface temperature (SST) thermal fronts in eastern Indonesian waters are strongly modulated by monsoonal winds and regional interactions. Previous studies have mainly focused on the northern Arafura Sea and the Banda Sea, where strong upwelling and large-scale circulation dominate. In contrast, the southwestern Arafura Sea relatively understudied, despite its shallow continental shelf and strong exposure to seasonal monsoonal winds and ENSO-related climate variability. This study investigated the spatial and temporal variability of SST thermal fronts in the southwestern Arafura Sea under contrasting monsoonal phases and ENSO conditions. OSTIA product used to calculate horizontal SST gradients as indicators of surface thermal fronts, while wind forcing was analyzed using ERA5 reanalysis data. The results indicate that monsoonal circulation exerts the primary control on the intensity and distribution of SST thermal fronts, with ENSO acting as a secondary modulator. During the Southeast Monsoon, stronger southeasterly winds and enhanced surface cooling generate more intense and widespread frontal activity, particularly during La Niña events. In contrast, frontal signatures weaken during the Northwest Monsoon, when wind forcing and upwelling are reduced. These findings highlight the combined influence of seasonal monsoonal forcing and large-scale climate variability on SST thermal front dynamics in the southwestern Arafura Sea.

Keywords: Sea surface temperature, thermal front, gradient analysis, ENSO, Arafura Sea

1 Introduction

The Arafura Sea, located between Papua and northern Australia, forms part of the Indonesian Seas system that connects the Pacific and Indian Oceans through the Indonesian Throughflow (ITF) [1]. As a semi-enclosed basin within the Maritime Continent, this region is highly dynamic and influenced by complex interactions between seasonal monsoon reversals, ocean–atmosphere coupling, and interannual climate variability, such as the El Niño–

* Corresponding author: bila.h13@outlook.com

Southern Oscillation (ENSO) [2, 3]. These processes play a crucial role in regulating the heat and mass exchange within the Indo-Pacific, making the Arafura Sea an important but relatively understudied component of the regional circulation system.

Seasonal wind regimes strongly control the spatial and temporal distributions of sea surface temperature (SST) and surface circulation in the Arafura Sea [4]. During the Southeast Monsoon (June–August), persistent southeasterly trade winds enhance surface cooling, drive coastal upwelling along the continental shelf, and increase the horizontal temperature gradients. In contrast, the Northwest Monsoon (December–February) is characterized by northwesterly winds that promote stratified warmer surface layers and weaker horizontal gradients [5, 6]. These alternating wind systems create favorable conditions for frontogenesis, where water masses with contrasting thermal properties converge to form thermal fronts. A thermal front develops when two water masses interact, resulting in a steep horizontal temperature gradient that can be readily detected using satellite-derived SST data [7]

Thermal fronts are narrow transition zones characterized by strong horizontal temperature gradients that separate distinct water masses [8, 9]. They are key indicators of physical and biogeochemical processes in the ocean, and are often associated with enhanced vertical mixing, convergence, and nutrient enrichment [10, 11]. In open-ocean environments, temperature gradients typically range from 0.05–0.2 °C/km for weak fronts to more than 0.5 °C/km for strong ones [9, 10]. However, the magnitude and persistence of these gradients can vary substantially, depending on the local hydrographic conditions and spatial scale.

Despite its physical significance, the frontal structure of the Arafura Sea remains poorly characterized. Previous studies have mainly focused on SST variability, monsoonal upwelling, and chlorophyll distributions [5, 13, 14, 15], whereas the direct relationship between monsoonal wind forcing and thermal front dynamics has received little attention [16, 17]. Moreover, fine-scale mapping of thermal fronts in this shallow tropical sea is constrained by the scarcity of long-term high-resolution SST observations.

Thermal fronts are commonly identified by applying a gradient threshold to SST fields and delineating zones of significant horizontal temperature contrasts. Thresholds such as 0.04 °C/km [12] or 0.5 °C/km [18] are often used to distinguish fronts from background variability. While this approach is effective in open-ocean settings with relatively stable stratification, its application in shallow, tidally mixed regions, such as the Arafura Sea, can be problematic due to strong spatial and temporal variability in SST gradients driven by tidal mixing, surface heating, and transient wind forcing. Thus, the use of a fixed threshold may underestimate or overestimate the true extent and strength of frontal zones.

To address these limitations, the present study adopts a relative-gradient approach that focuses on spatial and temporal changes in the SST gradient magnitude rather than applying a universal threshold. This method allows for a more adaptive identification of potential thermal front zones, capturing fine-scale frontal variability under dynamic hydrographic conditions. Furthermore, by analyzing data from three representative ENSO phases, this study investigated how large-scale climate variability modulates monsoonal influences on thermal front development. The results provide new insights into the mechanisms driving frontal variability in the southwestern Arafura Sea and contribute to a better understanding of ocean–atmosphere interactions within the eastern Indonesian seas.

2 Data and method

2.1 Study area

Observations were conducted to determine the presence and potential of a thermal front in the southwestern part of the Arafura Sea [longitude: 130°E – 132°E and Latitude: 7.8° S – 9.2°S)]. This region is directly influenced by the seasonal monsoon system and outflow of the Indonesian Throughflow (ITF). However, despite its important role as a transitional zone between the Pacific and Indian Oceans, studies on the occurrence and variability of thermal fronts in the Arafura Sea remain limited and require comprehensive investigation. Below (**Fig.1**) shows the study area with the station from the CTD observations, which one of the station will be used as validation for reanalysis data.

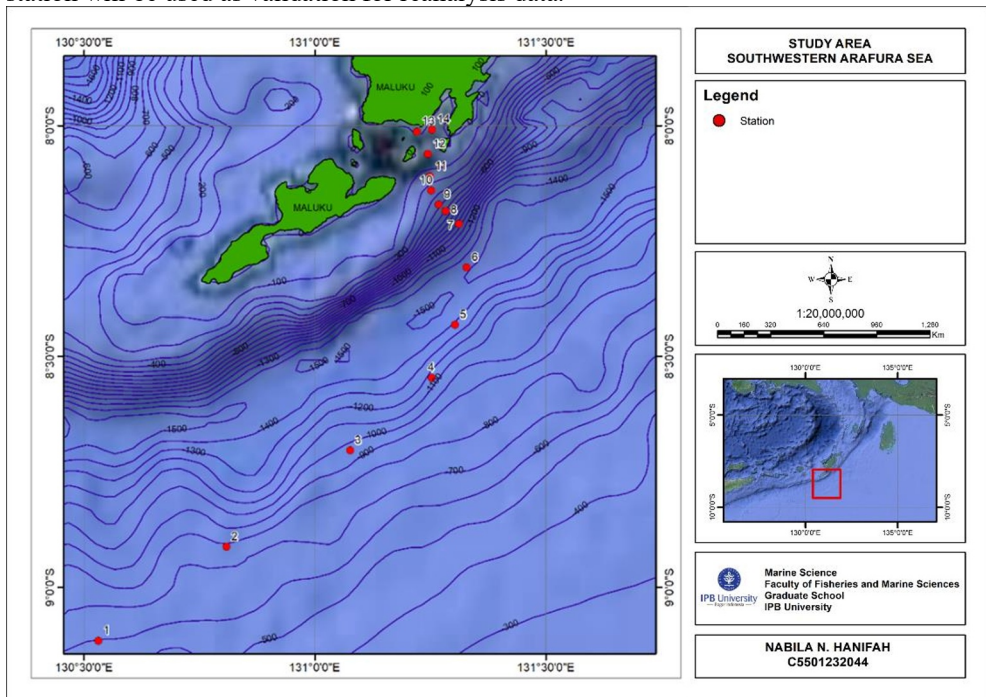


Fig. 1. Study area in southwestern Arafura Sea.

2.2 Data

The observation period occurred during the eastern monsoon, specifically from June to August, with a reference year based on the Niño index of 3.4. The years used were 2010 (La Niña), 2020 (normal), and 2015 (El Niño). The data used included Sea Surface Temperature (SST) data taken from the OSTIA product downloaded in NetCDF format through Copernicus Marine Environment Monitoring Service (CMEMS) with DOI: <https://doi.org/10.48670/moi-00165> in the form of daily data, which was then averaged over months with a resolution of $0.05^\circ \times 0.05^\circ$. There were also supporting data, such as wind in the form of vectors U_0 and V_0 downloaded in NetCDF format through CMEMS with a spatial resolution of 0.25° and the same resolution for the horizontal with DOI: <https://doi.org/10.48670/moi-00181>, as well as the wind resulting in the calculation of the magnitude of wind. The tools used in the processing and analysis of data in this study are

several programs, such as PyFerret, Python, and JupyterLab Notebook for visualization. All data were already validated with the CTD that was taken in the study area using Taylor Diagram Methods. From all CTD stations deployed during the survey, Station 7 was chosen for analysis. The standard deviations of the observed and reanalysis data were 6.99 and 7.37, respectively, indicating strong similarity and supporting the representativeness of the reanalysis dataset.

2.3 Method

Fronts were identified using gradients according to [19]. Based on a study by [20], the authors compared this method with other methods that apply different thresholds. In this technique, the magnitude of the spatial temperature gradient ($\text{Grad}_{x,y}$) is first calculated using the Kostiano approach as follows:

$$\text{Grad}_{x,y} = \sqrt{\left(\frac{\partial \text{SST}}{\partial x}\right)^2 + \left(\frac{\partial \text{SST}}{\partial y}\right)^2} \quad (1)$$

Previous studies suggested that SST gradients of $0.05^\circ - 0.2^\circ \text{C/km}$ typically indicate weak fronts, whereas gradients exceeding 0.5°C/km are the characteristic of strong coastal or shelf fronts [8, 9, 21]. However, in tropical open-ocean environments, such as in this study area, the temperature contrasts are generally smaller owing to strong vertical mixing and warm background SST [11]. Therefore, a relative gradient threshold ($<0.05^\circ \text{C/km}$) was applied to detect weak but spatially coherent thermal fronts, consistent with the scale of variability observed in similar tropical waters [17]. Meanwhile, for wind data, only vector plots were created to show the direction of the wind, which will be used to determine the temperature gradient that caused the front.

3 Result and discussion

3.1 Influence of wind variability

Seasonal wind variability plays a central role in shaping the formation and evolution of thermal fronts in southwestern Arafura Sea. The regional wind system is characterized by strong southeasterly trades during the Southeast Monsoon (June–August) and weaker northwesterly winds during the Northwest Monsoon (December–February). These alternating wind regimes modulate sea surface temperature (SST) gradients by altering the balance between surface cooling, vertical mixing, and horizontal advection [4, 5].

The wind field over the southwestern Arafura Sea exhibited distinct seasonal and interannual variability associated with the Asian–Australian monsoon system and ENSO phases (**Fig. 5**). During the Northwest Monsoon (December–February), the prevailing winds blow from the northwest, transporting warm, low-salinity waters from the Banda and Timor Seas toward the Arafura Sea. In contrast, during the Southeast Monsoon (June–August), the dominant southeasterly winds enhance surface cooling and coastal upwelling through Ekman divergence along the southern margin of the Arafura platform [11, 22].

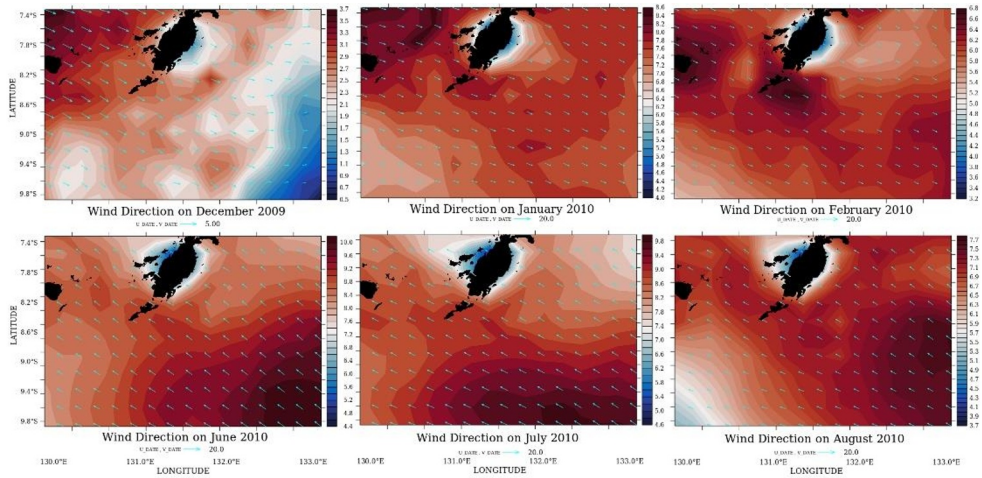


Fig. 2. Monthly wind direction and speed over the southwestern Arafura Sea during *La Niña* year 2010 (December 2009 – August 2010) derived from ERA5 reanalysis data. The southeasterly winds dominate during the Southeast Monsoon (June–August), while northwesterly winds prevail during the Northwest Monsoon (December–February).

In the *La Niña* year (2010), the wind intensity was relatively strong throughout both monsoonal phases, with enhanced southeasterly winds during the Southeast Monsoon (June–August) (**Fig. 2**). This pattern likely strengthened the surface cooling and increased SST gradient magnitudes, consistent with the enhanced heat flux and wind-driven mixing [11]. Conversely, during the *El Niño* year (2015), the southeasterly winds intensified further and persisted longer in the transition months (**Fig. 3**). The stronger southeasterly flow during El Niño suppresses warm-water advection from the north and amplifies cooling near the shelf edge, which supports the formation of thermal fronts [23, 24].

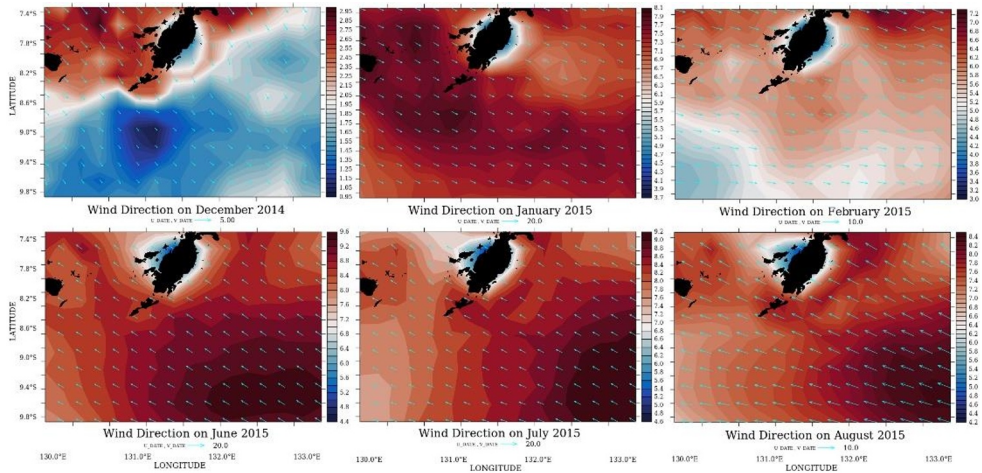


Fig. 3. Monthly wind direction and speed during *El Niño* year 2015 (December 2014 – August 2015). Weaker northwesterly winds during the Northwest Monsoon and intensified southeasterlies in the Southeast Monsoon period reflect the enhanced monsoonal contrast typically associated with El Niño conditions.

Meanwhile, the neutral-condition year (2020) displayed relatively weaker and less organized wind patterns (**Fig. 4**). The reduced wind forcing likely contributed to the weaker

horizontal SST gradients observed during this period, suggesting a diminished role of surface-driven mixing compared with ENSO years. A similar behavior has been observed across the eastern Indonesian seas, where the modulation of monsoonal winds by ENSO significantly alters the upper-ocean thermal structures [25].

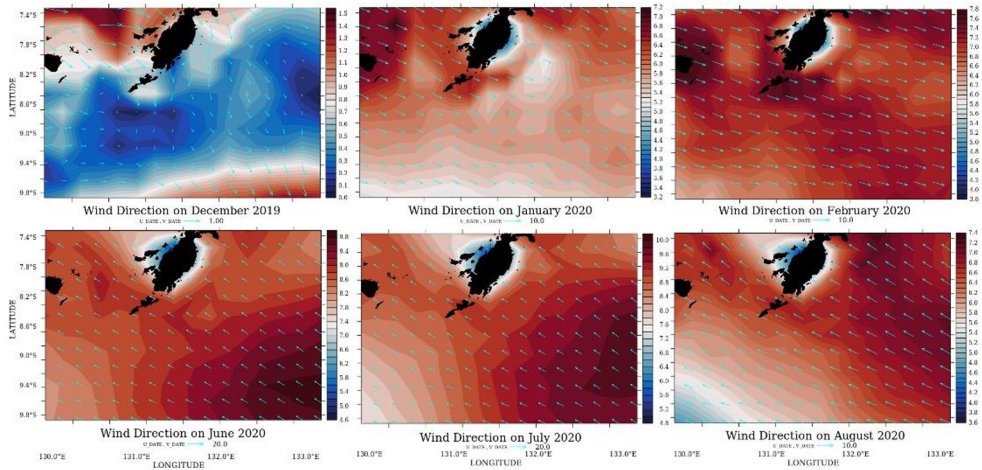


Fig. 4. Monthly wind direction and speed during *Normal* year 2020 (December 2019 – August 2020). Wind intensity and direction display a more transitional pattern between the monsoons, indicating weaker atmospheric forcing relative to ENSO years.

During the Southeast Monsoon, enhanced southeasterly winds drive offshore Ekman transport, leading to the divergence of surface waters and upwelling of cooler subsurface layers along the Arafura Shelf [6]. This process sharpens the horizontal temperature gradients and strengthens the thermal front signatures, particularly near the Saumlaki region and the western margin of the Arafura Sea. The strong correspondence between upwelling-favorable wind stress and elevated $|\nabla SST|$ values during this period indicates a wind-driven frontogenesis mechanism, consistent with regional circulation models [2].

Conversely, during the Northwest Monsoon, northwesterly winds promote the inflow of warm, low-salinity waters from the Banda and Timor Seas, resulting in a deepened thermocline and a reduced vertical temperature contrast. Under these conditions, SST gradients weaken ($<0.008\text{ }^{\circ}\text{C km}^{-1}$), and frontal features become less distinct. The spatial distribution of wind stress during this period (**Fig.7**) clearly illustrates the dominance of onshore wind components, which suppressed upwelling and thermal homogenization of the surface layer.

The ENSO further modulates these wind-driven processes. During La Niña, intensified southeasterly trades amplify upwelling and increase $|\nabla SST|$ magnitude, while El Niño years are marked by weakened winds and diminished frontal activity. This linkage between atmospheric forcing and the SST gradient structure underscores the dynamic coupling between local monsoon circulation and basin-scale ENSO variability. The sensitivity of the Arafura Sea to these wind anomalies highlights its role as a transitional zone within the Indo-Pacific system, where even modest shifts in wind direction or strength can alter the frontal intensity and distribution [2, 3].

3.2 Spatial and temporal distribution of thermal fronts

The spatial and temporal variabilities of the thermal fronts in the southwestern Arafura Sea exhibited distinct seasonal patterns and interannual modulation by ENSO events (**Fig. 5**).

During the Northwest Monsoon (December–February), the SST gradient magnitude ($|\nabla\text{SST}|$) remains weak ($<0.008\text{ }^{\circ}\text{C km}^{-1}$), indicating minimal surface temperature contrast due to intense stratification and weak wind stress. Westerly winds transfer warm surface water from the Banda Sea, suppressing vertical mixing and reducing the formation of horizontal thermal gradients. This seasonal pattern aligns with the deepened thermocline and warm surface layer previously observed during the monsoon reversal [4].

In contrast, during the Southeast Monsoon (June–August), $|\nabla\text{SST}|$ the areas increase, particularly along the continental shelf near Saumlaki and the western Arafura. Southeasterly trade winds enhance offshore Ekman transport and promote upwelling of cooler subsurface water, sharpening temperature contrasts and strengthening frontal zones [5, 6]. The observed patterns correspond to intensified wind-driven cooling and baroclinic adjustment, consistent with monsoon-related upwelling processes across the Banda–Arafura transitional zone [5, 4].

During the transition between monsoons, the response of thermal fronts is further influenced by the interplay between the local wind forcing and background oceanic variability associated with ENSO. The persistence of weak SST gradients during the Northwest Monsoon and their enhancement during the Southeast Monsoon suggests that regional frontogenesis is primarily wind-driven rather than buoyancy-controlled. However, variations in background stratification associated with ENSO can modulate this response. In the shallow Arafura Sea, wind-driven mixing and surface heat fluxes play a dominant role, while ENSO-related changes in subsurface structure may influence vertical temperature gradients without directly controlling upwelling efficiency [25]. This interaction between monsoon wind stress and ENSO-driven thermocline adjustment creates a temporally shifting frontal structure that governs thermal variability across the region. To illustrate the seasonal contrast in the thermal front distribution (**Fig. 5**), the monthly SST gradient magnitude ($|\nabla\text{SST}|$) during the 2009–2010 La Niña period was calculated. The figure clearly shows stronger and more extensive frontal zones during the Southeast Monsoon (June–August), whereas weaker gradients dominate during the Northwest Monsoon (December–February).

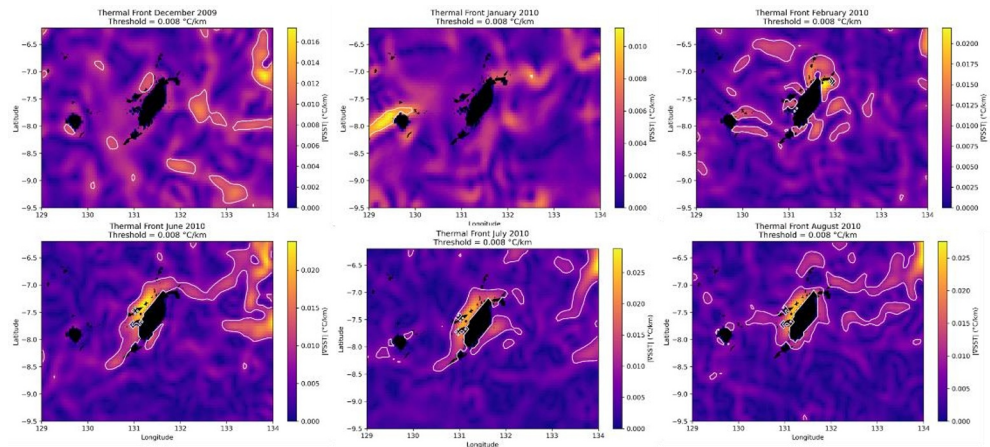


Fig. 5. Monthly distribution of sea surface temperature (SST) gradient magnitude ($|\nabla\text{SST}|$, $^{\circ}\text{C km}^{-1}$) in the southwestern Arafura Sea during December 2009 – August 2010 (La Niña period). Large area fronts gradients appear during the Southeast Monsoon (June–August), indicating enhanced frontal activity linked to upwelling and intensified southeast trades. Cooler gradients during December–February correspond to the Northwest Monsoon with weak mixing and warm stratified waters.

Interannual analysis revealed that the ENSO phases strongly modulate the strength and extent of the thermal fronts. During La Niña 2010, the enhanced southeast trade and shallower thermocline intensified upwelling and produced relatively stronger SST gradients along the southern shelf [11]. Conversely, El Niño 2015 weakened the trade and elevated

SSTs, leading to more diffuse fronts and a northward shift in frontal activity. Under neutral conditions in 2020, moderate frontal features reemerged, suggesting a transitional phase influenced by both local wind forcing and residual thermocline anomalies. This indicates that ENSO affects the regional energy balance and stratification, thereby altering the frontogenesis intensity across monsoon cycles.

The spatial pattern of the SST gradients during the 2014–2015 El Niño period (**Fig. 6**) contrasts markedly with the La Niña year. The gradients appeared more diffuse and weaker, suggesting that the anomalously warm and stratified surface layer during El Niño suppressed frontogenesis and vertical mixing in the region.

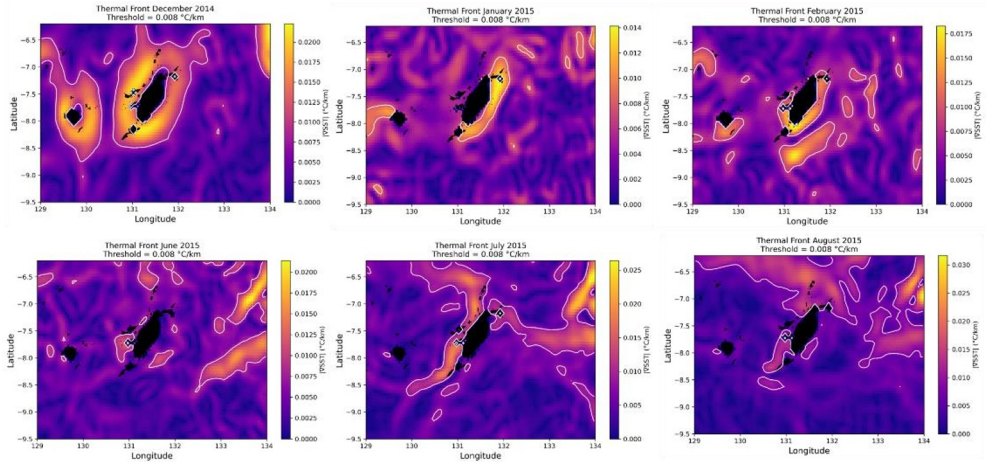


Fig. 6. Monthly distribution of SST gradient magnitude ($|\nabla SST|$, $^{\circ}\text{C km}^{-1}$) in the southwestern Arafura Sea during December 2014 – August 2015 (El Niño period). SST gradients weakened (< 0.008 $^{\circ}\text{C km}^{-1}$) relative to La Niña conditions, with fronts shifting northward and becoming more diffuse. Reduced trade-wind intensity and elevated SSTs suppress frontogenesis, consistent with El Niño-related thermocline deepening.

The shallow shelf geometry of the Arafura Sea facilitates intense vertical mixing, which tends to homogenize the upper water column and weaken the horizontal temperature contrasts. During the southeast monsoon (JJA), strong southeasterly winds enhance the Ekman divergence and localized upwelling along the shelf break [14]. However, this upwelling signal is often masked at the surface by turbulent mixing and rapid surface heating under high insolation, resulting in relatively subtle SST gradients compared to deeper oceanic upwelling zones, such as the Banda or Timor Seas [11, 26].

Furthermore, the frontogenesis mechanisms in the southwestern Arafura Sea are temporally modulated by the ENSO. During El Niño events, weakened northwest monsoon winds and reduced convective activity enhance SST and stratification differences across the shelf, occasionally sharpening frontal boundaries [10, 22]. Conversely, La Niña conditions intensify the northwest monsoon winds and freshwater inputs from the Aru and Papua regions, increasing the surface mixing and diminishing the horizontal temperature gradient.

Because of this high temporal variability, applying a fixed thermal front threshold (e.g., 0.04 $^{\circ}\text{C km}^{-1}$) may not accurately capture the evolving frontal patterns in such semi-enclosed tropical systems. Instead, this study adopted a relative-variability approach, emphasizing the spatial change in ∇SST to identify fine-scale fronts under variable forcing, thus, a threshold of 0.008 $^{\circ}\text{C km}^{-1}$ was selected after evaluating the regional ∇SST variability, ensuring that the identified fronts reflect the intrinsic thermal structure of the study area. This adaptive technique has proven effective for shelf seas with strong wind and tidal interactions, such as the Arafura and Timor Seas [23]. The SST gradient magnitudes in the Arafura Sea are weaker

than those typically reported in open-ocean environments, where gradients can exceed $0.5 \text{ }^\circ\text{C km}^{-1}$ [9, 12]. The relatively small gradients observed here ($<0.02 \text{ }^\circ\text{C km}^{-1}$) reflect the shallow bathymetry, strong tidal mixing, and transient wind forcing that characterize the Arafura shelf [15].

Overall, these findings emphasize that monsoon-driven wind stress, ENSO-related atmospheric variability, and tidal processes jointly regulate the formation and dissipation of the thermal fronts in the Arafura Sea. The weak yet dynamic gradients observed highlight the tight coupling between the surface processes and subsurface thermocline fluctuations, which are further modulated by cross-shelf exchange and boundary currents from the Banda Sea [11, 22].

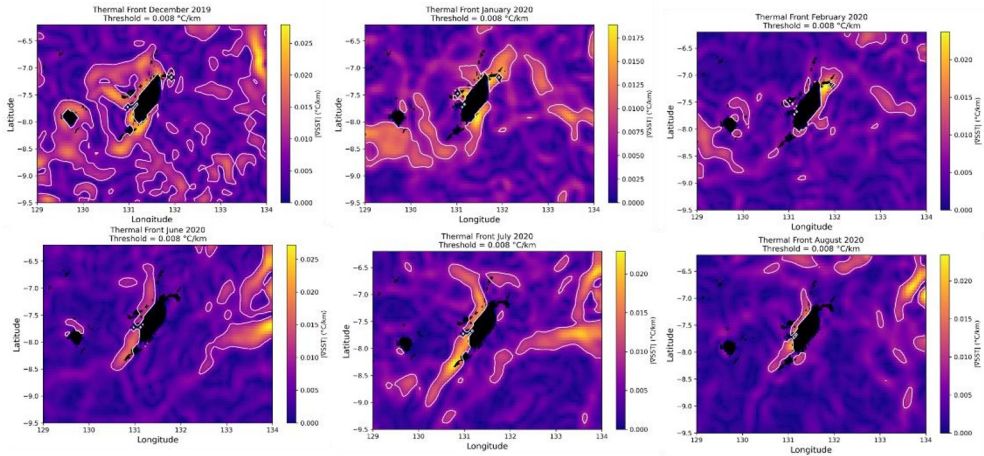


Fig. 7. Monthly distribution of SST gradient magnitude ($|\nabla\text{SST}|$, $^\circ\text{C km}^{-1}$) in the southwestern Arafura Sea during December 2019 – August 2020 (neutral to weak La Niña conditions). Moderate gradients ($0.008 \text{ }^\circ\text{C km}^{-1}$) reappear along the continental shelf near Saumlaki during the Southeast Monsoon, reflecting transitional wind forcing and partial recovery of upwelling intensity.

4 Conclusions

These findings reveal that wind variability plays an important role in modulating the thermal structure and circulation in the Arafura Sea. During the southeast monsoon, strong southeasterly winds enhance Ekman divergence and upwelling along the shelf, intensifying surface cooling and frontogenesis, whereas the northwest monsoon weakens these processes, allowing stratification to dominate. This monsoon-driven alternation governs the regional exchange between the Banda and Arafura Seas, linking local shelf dynamics to broader Indonesian Throughflow variability. These results emphasize that even subtle shifts in monsoon intensity can significantly influence the physical state and water mass distribution across this transitional oceanic system.

References

1. I. Buton, S. Tubalawony, M.C. Wattimena, Variabilitas Hidrometeorologi permukaan Laut Arafura pada saat fenomena ENSO. *J. Laut Pulau: Hasil Penelit. Kelautan* **2**, 32–50 (2023). <https://doi.org/10.30598/jlpvol2iss2pp32-50>
2. J. Sprintall, A.L. Gordon, A. Koch-Larrouy, T. Lee, J.T. Potemra, K. Pujiana, S.E. Wijffels, The Indonesian seas and their role in the coupled ocean-climate system. *Nat. Geosci.* **7**, 487–492 (2014). <https://doi.org/10.1038/ngeo2188>

3. A.L. Gordon, Large-scale effects of the Indonesian Throughflow. *Oceanography* **18**, 151–1623 (2005). <https://doi.org/10.5670/oceanog.2005.01>
4. A.S. Atmadipoera, A.A. Almatin, R. Zuraida, Y. Permanawati, Seasonal upwelling in the northern Arafura Sea from multi-datasets in 2017. *Pertanika J. Sci. Technol.* **28**, 1487–1515 (2020). <https://doi.org/10.47836/pjst.28.4.19>
5. W.S. Pranowo, Dinamika upwelling dan downwelling di Laut Arafura dan Timor. *Widyariset.* **15**, 415–424 (2012)
6. M. Zainuddin, S.I. Saitoh K. Saitoh, Detection of potential fishing ground for albacore tuna using synoptic measurements of ocean color and thermal remote sensing in the northwestern North Pacific. *Geophysical Research Letters*, **31**, L20311 (2004). <https://doi.org/10.1029/2004GL021000>
7. S. Panggabean, S. Mubarak, M. Ghalib, Penentuan daerah thermal front di Laut Timur Sumatera Provinsi Riau. *Jurnal Perikanan dan Kelautan*, **23**, 8–14 (2018)
8. J.J. Simpson, On the accurate detection and enhancement of oceanic features observed in satellite data, *Remote Sens. Environ.* **33**, 17–33 (1990). [https://doi.org/10.1016/0034-4257\(90\)90052-N](https://doi.org/10.1016/0034-4257(90)90052-N)
9. D.S. Ullman, P.C. Cornillon, Satellite-derived sea surface temperature fronts on the continental shelf off the northeast U.S. coast. *J. Geophys. Res.* **104**, 23459–23478 (1999). <https://doi.org/10.1029/1999JC900133>
10. I.M. Belkin, P.C. Cornillon, K. Sherman, Fronts in large marine ecosystems. *Prog. Oceanogr.* **81**, 223–236 (2009). <https://doi.org/10.1016/j.pocean.2009.04.015>
11. K. Sun, J. Chong, L. Diao, Z. Li and X. Wei, On the use of ocean surface doppler velocity for oceanic front extraction from Chinese Gaofen-3 SAR Data. *IEEE Journal of Selected Topics in Applied Earth Observations and Remote Sensing*, **15**, 2709–2720 (2022) <https://doi.org/10.1109/JSTARS.2022.3162445>
12. I.M. Belkin, J.E. O'Reilly, An algorithm for oceanic front detection in chlorophyll and SST satellite imagery. *J. Mar. Systems.* **78**, 3, (2009). <https://doi.org/10.1016/j.jmarsys.2008.11.018>
13. Y. Riupassa, and J. Wattimury, Variabilitas musiman suhu permukaan laut dan angin di Laut Arafura. *Jurnal Laut Pulau: Hasil Penelitian Kelautan*, **1**, 71–84 (2022). <https://doi.org/10.30598/jlpvolliss2pp71-84>
14. M.C. Wattimena, S. Tubalawony, Variasi parameter oseanografi di utara Laut Arafura pada tahun super La Nina 2010 dan El Nino 2015. *Journal of Coastal and Deep Sea*, **1**, 42–50 (2023). <https://doi.org/10.30598/jcds.v1i1.11325>
15. J. Kämpf and P. Chapman, The functioning of coastal upwelling systems. *Upwelling systems of the world: A scientific journey to the most productive marine ecosystems*, **1**, 31–65 (2016). https://doi.org/10.1007/978-3-319-42524-5_2
16. S.C. Bernardes, K. von Rintelen, T. von Rintelen, A.R. Pepato, T.J. Page, Ecological changes have driven biotic exchanges across the Indian Ocean. *Sci. Rep.* **11**, 23357 (2021). <https://doi.org/10.1038/s41598-021-02799-7>
17. T.K.E Mahardhika, G. Harsono. Studi eddy di Laut Arafuru menggunakan data altimetri tahun 2018. *J. Hidrografi Indones*, **4**, 79–86 (2022). <https://doi.org/10.62703/jhi.v4i2.34>
18. M. Kahru, E. Di Lorenzo, M. Manzano-Sarabia, B. Greg Mitchell, Spatial and temporal statistics of sea surface temperature and chlorophyll fronts in the California Current. *J. Plankton Res.* **34**, 749–760 (2012). <https://doi.org/10.1093/plankt/fbs010>

19. A.G. Kostianoy, A.I. Ginzburg, M. Frankignoulle, B. Delille, Fronts in the Southern Indian ocean as inferred from satellite sea surface temperature data. *Journal of Marine Systems*, **45**, 55–73 (2004). <https://doi.org/10.1016/j.jmarsys.2003.09.004>
20. M. Jishad, N. Agrawal, Thermal front detection using satellite-derived sea surface temperature in the Northern Indian Ocean: Evaluation of gradient- based and histogram-based methods, **50**, 1291–1299 (2022). <https://doi.org/10.1007/s12524-022-01527-6>
21. I.M. Belkin, P. Cornillon, SST fronts of the pacific coastal and marginal seas. *Pacific Oceanography*, **1**, 90–113 (2003)
22. K. Wyrtki, *Physical oceanography of the Southeast Asian waters* (University of California, Scripps Institution of Oceanography, La Jolla, California, 1961)
23. A.L. Gordon, R.A. Fine, Pathways of water between the Pacific and Indian oceans in the Indonesian Seas. *Nature* **379**, 146–149 (1996). <https://doi.org/10.1038/379146a0>
24. F. Syamsudin, H.M. van Aken, A. Kaneko, Annual variation of the southern boundary current in the Banda Sea. *Dynamics of atmospheres and oceans*, **50**, 129–139 (2010). <https://doi.org/10.1016/j.dynatmoce.2009.12.005>
25. J. Sprintall, A. Révelard, The Indonesian throughflow response to Indo-Pacific climate variability. *Journal of Geophysical Research: Oceans*, **119**, 2, 1161–1175 (2014). <https://doi.org/10.1002/2013JC009533>
26. S. Kida, S. Wijffels, The impact of the Indonesian Throughflow and tidal mixing on the summertime sea surface temperature in the western Indonesian Seas. *J. Geophys. Res. Oceans*. **117**, C09007 (2012). <https://doi.org/10.1029/2012JC008162>
27. H. Andruleit, Status of the Java upwelling area (Indian Ocean) during the oligotrophic northern hemisphere winter monsoon season as revealed by coccolithophores. *Mar. Micropaleontol.* **64**, 36–51 (2007), <https://doi.org/10.1016/j.marmicro.2007.02.001>